CHEMICAL BATH DEPOSITION AND MICROSTRUCTURING OF TIN (II) SULFIDE FILMS FOR PHOTOVOLTAICS

Steven M. Herron[a], Artit Wangperawong[b], Stacey F. Bent[c]
[a] Department of Chemistry, Stanford University, Stanford, CA, U.S.A.
[b] Department of Electrical Engineering, Stanford University, Stanford, CA, U.S.A.
[c] Department of Chemical Engineering, Stanford University, Stanford, CA, U.S.A.

ABSTRACT

Tin (II) sulfide is prepared through chemical bath deposition and annealed in a hydrogen sulfide environment to produce thin films for photovoltaic devices. The grain size, composition, and morphology are controlled by tailoring the bath composition and annealing conditions. The films have stoichiometric composition, are oxygen-free, have an optical band gap below 1.2 eV, and have an orthorhombic crystal structure. Through this method, a variety of film morphologies can be deposited, from dense films to micro-crystalline porous materials, in which micro-structured platelets can be incorporated through a self-assembly process. Annealing treatments simultaneously increase crystal size and improve purity to more efficiently extract photo-generated carriers. Electronic properties of the films are presented as well as insights into device preparation.

INTRODUCTION

Rapid advances in renewable energy technology and implementation will be needed in the next several decades in order to ensure a smooth transition away from fossil fuels and nuclear energy, which comprised about 93% of the world's energy budget in 2010, the balance supplied by hydroelectric power, with a negligible contribution from solar energy [1]. The current high costs of silicon processing and relative scarcity of indium and tellurium limit the terawatt-scale deployment of silicon, CdTe, and CIGS photovoltaics, allowing other materials to stake their claim in the future energy economy.

Among these possible materials is tin (II) sulfide, SnS, a non-toxic, abundant, p-type absorber well matched for solar absorption with an indirect bandgap of 1.1 eV and a high absorption coefficient above 1.3 eV [2,3]. Recently, SnS thin films have been deposited for photovoltaic and photoelectrochemical applications by several techniques: spray pyrolysis, electrodeposition, chemical bath deposition, and vacuum evaporation; furthermore devices have been reported as stable over time [3-6]. With a simpler stoichiometry than the attractive $Cu_2ZnSn(S,Se)_4$ kesterite-family of absorbers[7] and its incomplete exploration as a photovoltaic absorber, it could be a promising material for large-scale development [8]. Chemical bath deposition, the technique used here, is a low-cost, scalable, aqueous deposition method widely used for CdS buffer layers that has the potential to deposit absorber materials as well, making it amenable to the production of completely solution-deposited devices [5,9].

Spray pyrolysis has yielded the highest efficiency in SnS-absorber photovoltaics so far, with 1.3% achieved in a SnS-CdS junction. Limitations were attributed to shunting and series resistance as well as recombination at the junction and a thin absorber; other efficiencies have been below 1% [3]. However, there is little evidence presented to indicate long-range crystal order extending from the back contact to the heterojunction, a necessary component of efficient cells. Furthermore, detailed elemental analyses have rarely been reported alongside device characterization, whereas several of the aforementioned deposition techniques have the potential to introduce carbon, nitrogen, and oxygen impurities into the film. Annealing of SnS films has been conducted largely in nitrogen and air, which may not be sufficient to remove oxygen impurities, and would likely introduce oxygen in some cases.

In the present work, we report studies on chemical bath deposition (CBD) of SnS and subsequent annealing in a hydrogen sulfide environment to achieve increases in crystallinity and control over morphology and composition. In altering the bath and annealing conditions, we demonstrate micro-structuring of the absorber layer for enhanced photon collection efficiency. Preliminary solar cell devices were fabricated to show that this material is applicable in earth-abundant, non-toxic thin film photovoltaics.

EXPERIMENTAL

SnS was grown at temperatures from 20-50°C on glass and molybdenum-coated silicon substrates through a method based on that of Nair et al. [10]. The substrates were cleaned using acetone, ethanol, and de-ionized water and then mounted in the CBD bath containing acetone, $SnCl_2$, triethanolamine(TEA), aqueous ammonia, and thioacetamide. By adjusting the bath conditions, different film morphologies were obtained, from dense films at low TEA concentrations to porous films at high TEA concentrations, with film thicknesses up to 600 nm. The CBD procedure was repeated to yield as-deposited thicknesses over 1 micron.

These samples were annealed in a tube furnace with 10% H_2S (balance H_2) gas or N_2 gas (control) flowing at temperatures from 300-600°C. Complete device architectures were fabricated with the addition of atomic-layer-deposited- CdS and ZnO-Al:ZnO transparent conductive oxide [11,12].

The films were characterized by scanning electron microscopy (SEM), Auger electron spectroscopy (AES), X-ray diffraction (XRD), X-ray photoelectron spectroscopy (XPS) and transmission UV-Vis absorption spectroscopy. Resistivity and Hall measurements were made with a four-point probe. Ohmic contacts were prepared with indium, as reported [13], and were confirmed by a linearity check.

RESULTS AND DISCUSSION

AES and XPS indicated that the film composition as-deposited was SnO_xS_{1-x} and $SnO_{1+y}S_{1-y}$ on the surface. Upon H_2S annealing at all temperatures, the films were converted completely to SnS with a Sn:S ratio of 55(±5)%:45(±5)%, whereas nitrogen annealing left a substantial amount of oxygen in the films, as expected.

The XRD spectra of as-deposited and annealed CBD SnS films are displayed in Figure 1. The as-deposited films were nano-crystalline with an average coherence length of 9.5 nm estimated using the Scherrer relation:

$$T(nm) = \frac{0.9 \times 0.1541\, nm}{\Delta(2\theta) \times \cos(\theta)}$$

where 0.1541nm is the wavelength of Cu K_α radiation used in the XRD measurement, Δ(2θ) is the full-width-half-max in radians, and θ is in degrees. The crystal coherence length increased up to an average of 36 nm at 550°C for 30 min. All films were assigned as orthorhombic SnS, and an increase in both diffraction signal and peak sharpness is seen in higher temperatures in H_2S, and to a lesser extent in nitrogen, indicating an increase in crystallinity.

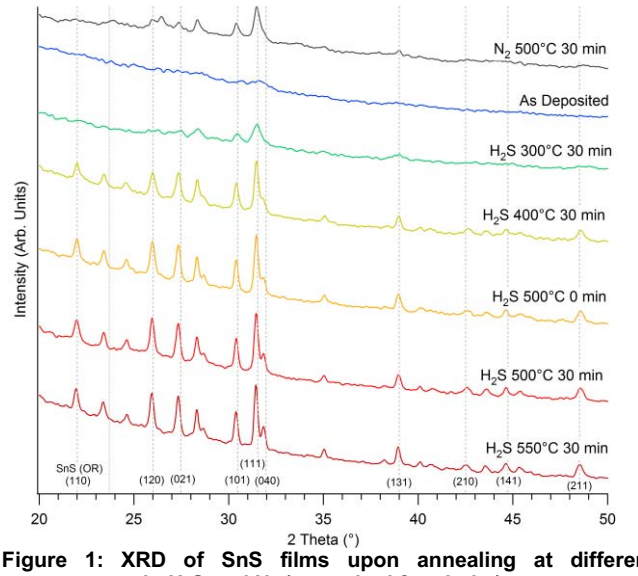

Figure 1: XRD of SnS films upon annealing at different temperatures in H_2S and N_2 (smoothed for clarity).

SEM images of cross-sections of the dense SnS films are depicted in Figure 2. These films are clearly polycrystalline with an estimated average grain size of several hundred nanometers. Electrical properties of these films are listed in Table 1. The high carrier concentration and relatively low mobility indicate that photovoltaic devices using these materials may benefit from a nano-structured interface [14].

Carrier Type	Holes
Resistivity (Ω*cm)	6.3 ± 0.1
Mobility ($cm^2V^{-1}s^{-1}$)	11 ± 7
Carrier concentration (cm^{-3})	$5*10^{16} – 3*10^{17}$

Table 1: Electrical properties of dense SnS films in Fig. 2

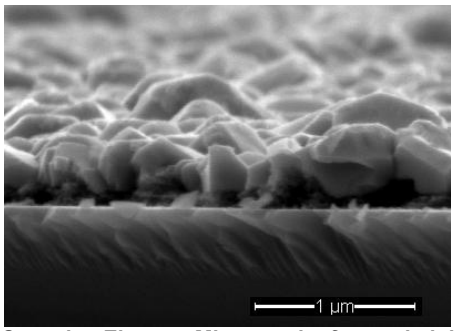

Figure 2: Scanning Electron Micrograph of annealed dense SnS films prepared by CBD and H_2S anneal.

The porous SnS samples are seen in Figure 3. The as-deposited films are about 1.2 micron thick and porous, with sharp bladed features confined to several nanometers in one direction. Above 400°C, the morphology appears to convert to crystallites several hundred nanometers across. The size of these features increases as annealing temperature increases in H_2S, consistent with the trends seen in XRD. In the N_2-annealed sample, this recrystallization does not take place, and the grain size cannot be larger than a couple tens of nanometers. A small decrease in film thickness accompanies anneals up to 500°C, followed by a significant decrease in nominal thickness at 550°C, which is accompanied by a growth of large vertically-oriented platelets of SnS out of the plane, as seen in Figure 4. The composition of these platelets is identical to that of the film, as confirmed by Auger electron spectroscopy.

The high aspect ratio and vertical orientation of these features makes them a potential candidate for micro-structured photovoltaic layers, in which the required minority carrier diffusion length can be decreased, at the cost of an increase in dark current. The size of the platelets is a function of temperature and annealing time, and can be controlled accordingly. When annealed for 2 hours at 550°C, platelets reached dimensions as large as 10 microns – see Figure 4.

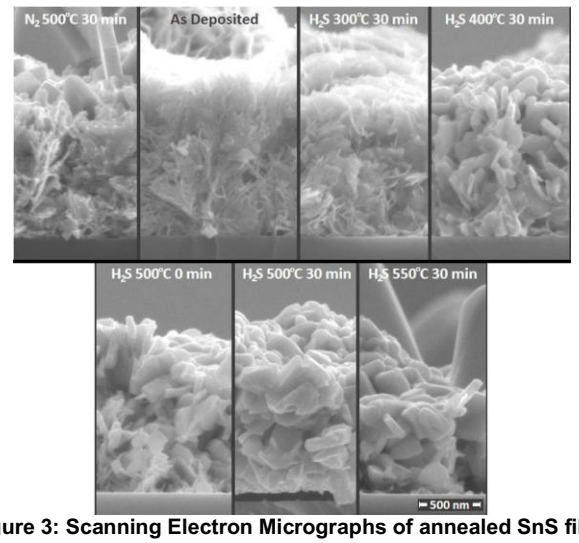

Figure 3: Scanning Electron Micrographs of annealed SnS films (scale bar = 500 nm).

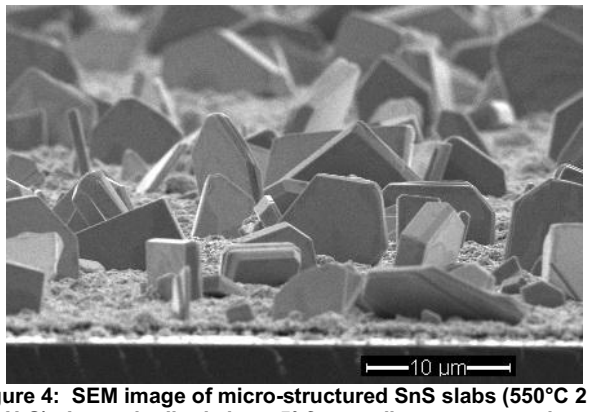

Figure 4: SEM image of micro-structured SnS slabs (550°C 2 hr. H_2S). Image is tilted about 5° from a direct cross-section.

UV-Vis data indicates an absorption onset around 750 nm, corresponding to an optical bandgap of about 1.65 eV for the as-deposited material, while the annealed materials exhibited both an indirect (allowed) transition at about 1.15 eV and a direct (allowed) transition at about 1.35 eV, as the $(\alpha h\nu)^n$ vs. photon energy plots showed linear regions extrapolating to these values, (Figure 5), (where n=2 for direct and 1/2 for indirect) [15]. These results are consistent with the conversion to SnS [4, 16] although these transition energies can only be considered estimates, as scattering was ignored in these transmission measurements.

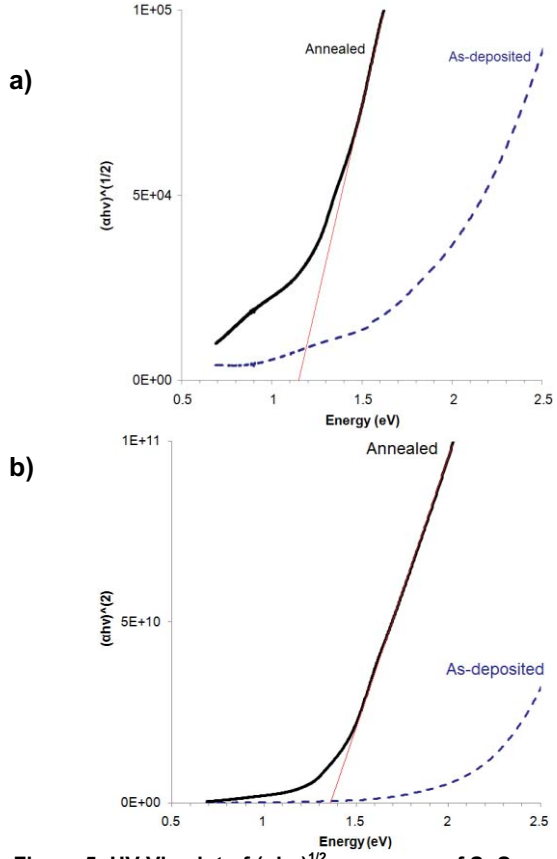

Figure 5: UV-Vis plot of $(\alpha h\nu)^{1/2}$ vs. energy of SnS samples on glass before and after annealing.

Several solar cell devices were fabricated to compare the behavior of the micro-structured SnS versus that of a planar SnS absorber; however the molybdenum substrate no longer provided low-resistivity contacts, and therefore photovoltaic performance has not yet been assessed. It was observed by Auger electron spectroscopy depth profiling that sulfur penetrated through the entire Mo film after the H_2S anneal. Figure 5 shows the AES depth profile of a region of one cell that was masked during SnS deposition but exposed to CdS and ZnO deposition. Sulfur penetration is evident throughout all of the molybdenum, and the partial conversion of Mo to MoS_2 is suggested as the cause for loss of conductivity. We aim to address this in future work through the selection of different substrates and less harsh annealing conditions.

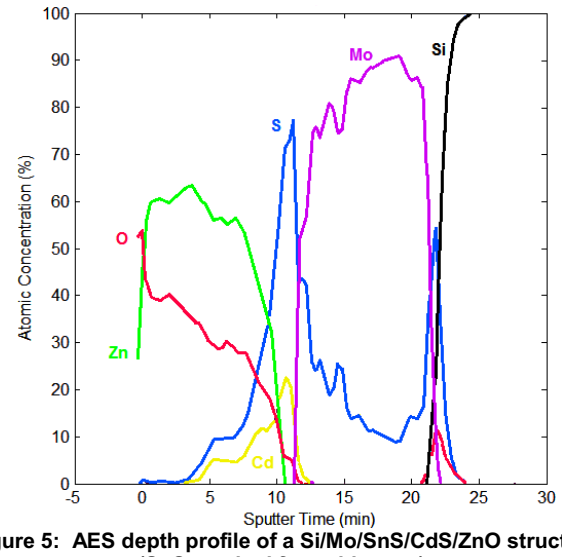

Figure 5: AES depth profile of a Si/Mo/SnS/CdS/ZnO structure (SnS masked from this area).

SUMMARY OF WORK

We present a study on the chemical bath deposition and subsequent annealing of SnS thin films as photovoltaic absorbers. Through control of bath composition and annealing conditions in this scheme, we are able to more carefully ensure the quality of the films as well as study micro-structuring in a low-cost, solution based method. The films deposited were nano-crystalline Sn(O,S) and converted to SnS of orthorhombic structure with increased crystal coherence length and the desired composition upon annealing in a hydrogen sulfide atmosphere as evidenced by Auger, XRD, SEM, and UV-Vis. The vertically-oriented platelets obtained appear to be highly crystalline, and characterization is under way to determine this. Initial device structures have been formed, with suggestions for improvement of back contact connections.

SIGNIFICANCE OF WORK TO PHOTOVOLTAICS

The success of SnS as an abundant, non-toxic photovoltaic absorber layer is predicated on the ability to deposit material with good crystallinity and interfaces. The purpose of these fundamental studies is to investigate how well this material

can perform in photovoltaic devices when the crystallinity, composition, and morphology are carefully monitored. The necessity of a sulfide annealing atmosphere and the benefits of micro-structuring are important issues to determine in this system. We also work to assess the feasibility of preparing efficient devices from a low-cost and scalable method such as chemical bath deposition with the eventual possibility of an all-solution-based synthesis.

ACKNOWLEDGMENTS

Studies were carried out as part of the Center on Nanostructuring for Efficient Energy Conversion, an EFRC funded by the U.S. Department of Energy, Office of Basic Energy Sciences under Award No. DE-SC0001060. Financial support from the National Science Foundation under Grant No. CBET 0930098 for the microstructure analysis is also acknowledged.

REFERENCES

[1] BP Statistical Review of World Energy (2010).

[2] P. Nikolic, S. Vujatovic: *Proc. 12th Int. Conf. Phys. Semicond.* Stuttgart (1974), **331**.

[3] N. Reddy, K. Reddy, R. Miles. *Solar Energy Materials & Solar Cells.* **90** (2006) 3041-3046

[4] B. Subramanian, C. Sanjeeviraja, M. Jayachandran: *Solar Energy Materials and Solar Cells*. **79** (2003) 57-65

[5] D. Avellaneda, M.T.S. Nair, P.K. Nair, *Thin Solid Films* **517** (2009) 2500-2502.

[6] H. Noguchi, A. Setiyadi, H. Tanamura, T. Nagatomo, O. Omoto, *Solar Energy Materials and Solar Cells* **35** (1994) 325-331.

[7] D. Mitzi, O. Gunawan, T. Todorov, K. Wang, S. Guha, *Solar Energy Materials & Solar Cells* **In Press** (2011)

[8] S. Habas, H. Platt, M. van Hest, D. Ginley, *Chem Rev.* (2010) **110** (**11**), 6571-6594.

[9] D. Avellaneda, M.T.S. Nair, P.K. Nair, *Mater. Res. Soc. Symp. Proc*. (2007) Vol. **1012**-Y12-29

[10] M. T. S. Nair, P. K. Nair, P. K. Nair, *Semicond. Sci. Technol*. **6** (1991) 132.

[11] Bakke, J.R.; Jung, H. J.; Tanskanen, J.T.; Sinclair, R; Bent. S.F. *Chemistry of Materials* (2010), **22**, 16.

[12] Tanskanen, J.T.; Bakke, J.R.; Pakkanen, T.A.; Bent, S.F. *Journal of Vacuum Science & Technology* **29**, 31507, (2011)

[13] Devika, M; Reddy, N.K.; Patolsky, F; Gunasehkar, K.R, *J. Appl. Phys.* **104** 124503, (2008)

[14] Wangperawong, A; Bent, S.F. *Appl. Phys. Lett.* **98**, 233106, (2011)

[15] Tauc, J; Menth, A; Wood, D.L., *Phys. Rev. Lett*, **25**, (1970)

[16] Johnson, J.B.; Jones, H.; Latham, B.S.; Parker, J.D.; Engelken, R.D.; Barber, C. *Semicond. Sci. Technol.* **14** (1999)